Journal of Theoretical and Applied Information Technology
15st July 2026. Vol.104. No.13

ISSN: 1992-8645 www.jatit.org E-ISSN: 1817-3195

AN INTELLIGENT NSNT-QRNN FRAMEWORK FOR AUTOMATED STAGE-WISE PANCREATIC CANCER DETECTION AND CLASSIFICATION FROM CT IMAGES

DHISHYA. E[1], ANANDABABU. P[2]

[1]Research Scholar, Department of Computer and Information Science,
Annamalai University, Chidambaram, Tamil Nadu, India,
[2]Assistant Professor/ Programmer, Department of Computer and Information Science,
Annamalai University, Chidambaram, Tamil Nadu, India,

Email ID: [1]dhishyadhishya@gmail.com, [2]drpabcud@gmail.com

ABSTRACT

One of the deadliest and most aggressive types of cancers, pancreatic cancer has historically been difficult to diagnose and treat because it is typically detected when it reaches a late stage, and there are limited options for treatment. As such, there is an urgent need to develop novel methodologies to provide earlier detection and enable radiologists to make informed decisions about patient care. To meet this demand, a fully automatic stage-wise pancreatic cancer disease detection and classification model has been proposed. This approach uses a Quasi-Recurrent Neural Network (QRNN), specifically designed to use NasNet-based architectures with a Quasi-Recurrent Neural Network. The NasNet-based architectures used within our proposed methodology are capable of extracting hierarchical deep features from CT scan images. These features are learned through the process of training on large amounts of labelled data. These deep features are then fed into a Quasi-Recurrent Neural Network (QRNN). It uses both convolutional and recurrent layers. These layers enable the QRNN to learn how to associate information across time. The association capabilities provided by the quasi-recurrent layers allow the QRNN to identify relationships between input information. The proposed framework consists of three main components. Initially, a pre-processing technique - the Wiener filter was used to reduce the image's noise. Secondly, Contrast-Limited Adaptive Histogram Equalization (CLAHE) was used to enhance the contrast of CT images. Following that, the TransUNet model was used to segment pancreatic tumors. The Quasi-Recurrent Neural Network is trained to classify pancreatic tumors based on their stage. The effectiveness of the proposed methodology is assessed through a comparative analysis with other state-of-the-art methodologies. Results show that the proposed framework provides a classification accuracy of 98.90% and performs better than previously reported methodologies.

Keywords: *Deep Learning, Pancreatic Disease, NasNet Segmentation, Computed Tomography, Image Processing*

1. INTRODUCTION

Pancreatic cancer is considered one of the biggest global public health threats due to its very high mortality and poor prognosis. Pancreatic cancer is well known to be one of the most aggressive types of cancer, and it also has a relatively low five-year survival rate compared to many other forms of cancer [1]. Pancreatic ductal adenocarcinoma (PDAC) is the most common type of pancreatic cancer and represents the vast majority of all pancreatic cancers. One of the main reasons why pancreatic cancer has such a high mortality rate is that the cancer is usually diagnosed late in the course of the disease. When pancreatic cancer is diagnosed late in the course of the disease, there are fewer viable treatment options available, and the chance of successfully treating the cancer decreases. Thus, accurately identifying the stages of pancreatic cancer early in the course of the disease will help clinicians treat patients more successfully and ultimately increase their chances of survival [2]. The development of pancreatic cancer occurs in several stages. Initially, pancreatic cancer develops

from small cellular and structural alterations within the pancreas. These cellular and structural changes will evolve into premalignant lesions, local tumours, and then eventually invasive cancer. Because the morphologic changes in the pancreas occur early in the disease process and are slight and difficult to detect visually, clinicians do not routinely observe them during the initial stages of the disease [3]. As the disease progresses, tumours may grow larger and extend beyond the confines of the pancreas. The precise staging of the disease is important, as each stage of the disease requires a unique set of treatments, including surgery, chemotherapy, and/or radiation therapy.

Therefore, the development of an automatic system that can accurately classify pancreatic cancer into various stages would greatly aid in the improvement of diagnostic accuracy and in initiating early medical interventions. Imaging is a key component of the diagnosis and management of pancreatic cancer. Of all of the imaging modalities available, computed tomography (CT) scans are the most commonly used method of imaging pancreatic cancer [4]. This is largely due to the fact that CT scans offer high spatial resolution and rapid image acquisition. Additionally, CT scans enable clinicians to visualize the pancreas in detail from multiple angles. CT scans allow clinicians to assess tumour size, anatomical location, vascular involvement, and the presence of metastasis. Although CT scans offer several advantages in the detection and diagnosis of pancreatic cancer, there are still limitations to the use of CT imaging. The pancreas is anatomically complex and has varying levels of signal intensity depending on the stage of disease [5]. For example, early-stage abnormalities or small lesions may be difficult to detect; thus, the visual assessment of CT scans by a clinician may be subject to variable levels of observer agreement and diagnostic fatigue. Due to these limitations, there is a significant need for intelligent computer-assisted diagnostic (CAD) systems to assist radiologists in providing a more accurate and reproducible diagnosis. Recent developments in both machine learning (ML) and deep learning (DL) have enabled researchers to develop increasingly sophisticated CAD systems for analyzing medical images.

Specifically, convolutional neural networks (CNNs) have demonstrated exceptional capabilities in learning hierarchical and discriminative features from large volumes of medical imaging data. CNN-based models are capable of automatically detecting, segmenting, and classifying abnormalities in medical images without requiring extensive handcrafted feature design. However, previous studies that utilize DL to analyze medical images have generally focused on binary classification tasks (e.g., distinguishing between normal and malignant tissue) instead of multi-class classification tasks. An additional challenge to achieving optimal performance in DL models is selecting the appropriate hyperparameters. Hyperparameters include parameters such as the learning rate, batch size, network depth, optimizer selection, and convolutional kernel dimensions [6]. All of these hyperparameters have significant effects on the model's convergence and generalization capabilities. If the hyperparameters are selected improperly, the model may suffer from overfitting, underfitting, or even unstable training. Therefore, selecting optimal hyperparameters is a critical aspect of designing robust and reliable DL-based frameworks for multi-stage pancreatic cancer detection and classification.

Motivated by these clinical and technical challenges, this research presents an innovative intelligent DL-based framework for automatic multi-stage pancreatic cancer detection and classification based on CT images. To develop and evaluate the proposed framework, this study utilized a dataset of CT images obtained from a publicly accessible database provided by Kaggle. In this research, the pancreatic cancer conditions were classified into four distinct stages: Normal (Healthy), Early Abnormality (Begin), Premalignant (Pre-Malignant), and Cancerous (Malignant). The proposed system was designed to integrate advanced pre-processing techniques, accurate segmentation of the pancreas, deep transfer-learning-based feature extraction, and optimized classification algorithms to effectively distinguish between these four stages. Through the implementation of a multi-stage classification strategy, the proposed system was intended to contribute to earlier detection, enhanced diagnostic accuracy, and a support tool for clinicians in making informed decisions regarding the diagnosis and treatment of pancreatic cancer.

The rest of this paper is organized as follows: Section 2 presents a review of the relevant literature on pancreatic cancer detection and classification using medical imaging technologies. Section 3 outlines the details of the proposed NSNT-QRNN methodology, including the pre-processing, segmentation, feature extraction, and classification components. Section 4 presents the experimental results and evaluation of the performance of the

proposed framework. Finally, Section 5 summarizes the findings of the study and identifies potential areas of future investigation.

2. RELATED WORKS

In [7], the author suggested a new Sparrow Search Algorithm with Stacked Deep Learning (SSASDL-PCDC) for the detection of pancreatic cancer based on CT images. The SSASDL-PCDC technique employs HHO with DenseNet for the extraction of features from images and a CNN-BiLSTM model for the classification of tumours. In addition, the algorithm utilizes the Sparrow Search Algorithm to optimize hyperparameters. Using this novel method, researchers were able to obtain a maximum accuracy of 99.26%. Although the model achieved high classification accuracy, it primarily focused on tumour detection and did not address stage-wise pancreatic cancer classification, which is crucial for clinical decision-making.

In [8], the author proposed a new, integrated deep learning method that was used for the segmentation and classification of tumours in CT images. For the segmentation of tumours, the authors utilized an Enhanced UNet model. They also developed a modified version of the ResNeXt model, which they utilized to classify tumours based on their stage (benign or malignant). Using the Tunicate Swarm Optimization technique, the authors were able to improve the accuracy of classification achieved by the modified ResNeXt model to 99.85%. These results demonstrate that the proposed method can be successfully used for the reliable detection of pancreatic cancer. However, the study considered only Benign and Malignant categories, thereby limiting its applicability to comprehensive multi-stage pancreatic cancer diagnosis.

In [9], the author presented a systematic method for the monitoring, forecasting, and classification of pancreatic tumours. As stated previously, the proposed model combines the advantages of both DNN technology and algorithms inspired by natural phenomena. Through the use of BAT-ML image segmentation on a CT dataset to find pancreatic tumours in medical images taken during CT scans, the proposed model demonstrated superior performance to the above-described models. Moreover, through achieving a classification accuracy of 99.61%, the proposed model demonstrated superior performance when compared to existing models.

In [10], the author proposed an Antlion Optimization (ALO)-based CNN-GRU (ALO-CNN-GRU) model for the segmentation and classification of tumours found in CT images. The proposed method consisted of a series of steps. First, a hybrid filter based on a combination of a Gaussian filter and a median filter was applied to the CT images to enhance image quality. Next, the ALO algorithm was employed to segment the tumours from non-tumour tissue. Finally, the segmented images were classified into either benign or malignant using a CNN-GRU model. Overall, the proposed model achieved an accuracy of 99.92%. Despite its promising performance, the optimization and segmentation procedures increase computational complexity, which may affect scalability and real-time clinical deployment.

Author [11] proposed a hybrid deep learning model for the classification of pancreatic cancer using CT and MRI images. Specifically, the authors employed a convolutional neural network (CNN)-based feature extraction (ResNet and EfficientNet) combined with machine learning (SVM and Random Forest) classifiers. The proposed model demonstrated better generalizability than traditional deep learning models and achieved an accuracy of 95%. Nevertheless, the framework focused primarily on classification performance and did nt incorporate dedicated pancreas segmentation to improve region-specific feature learning.

In [12], the author employed some computational methods for the automatic recognition and segmentation of pancreatic malignant tumours in CT images. The authors employed Convolutional Neural Networks (CNNs) and advanced deep learning techniques to develop a comprehensive method for the automated detection of pancreatic cancer.

Author [13] employed some recent-generation architectures and their improved versions, including combinations of these structures at both classifier and decision-making levels, to achieve a classification performance of over 98%. This paper proposes an end-to-end model for pancreatic cancer classification (ETEPCC-MDTL) using CT images. The ETEPCC-MDTL model consists of several steps. First, the authors applied a bilateral filter and an entropy-based segmentation technique to the CT images to segment the pancreas and remove background noise. Second, the authors employed a NASNet model optimized using the CSO technique to extract features from the segmented images. Third, the authors employed an Ensemble Network (ENN) optimized using the GSO technique to classify the extracted features. Overall, the

proposed model demonstrated good performance in terms of classification accuracy.

In [14], the author presents a complete, end-to-end deep learning model for the diagnosis of pancreatic tumours based on CT images. The proposed model is composed of four stages: image screening, pancreas localization, segmentation, and tumour diagnosis. Unlike previous models, the proposed model does not require any manual pre-processing of the original CT images. Instead, the system automatically pre-processes the original CT images. In addition, the proposed model demonstrated excellent performance in terms of classification accuracy, achieving an accuracy of 82.7%, an F1 score of 88.5%, and an Area Under Curve (AUC) of 0.871. Although the framework provided an end-to-end solution, its classification accuracy remained lower than that reported by several recent DL approaches.

Although existing DL frameworks have achieved encouraging results for pancreatic cancer detection, several limitations remain. Most studies focus on binary classification rather than stage-wise categorization. Furthermore, many approaches rely solely on CNN-based architectures that may not effectively capture long-range contextual dependencies. Several methods also employ conventional segmentation techniques that may fail to isolate pancreatic regions from surrounding tissues accurately. In addition, limited attention has been given to integrating advanced segmentation, automated feature extraction, and efficient sequential classifiers within a unified framework. These limitations motivate the deployment of the proposed NSNT-QRNN framework, which combines TransUNet-based segmentation, NASNet feature extraction, and QRNN classification to improve stage-wise pancreatic cancer diagnosis.

3. THE PROPOSED WORK

The Proposed NSNT-QRNN model follows a systematic and efficient workflow, as depicted in Fig. 1. The process begins with an image refinement performed by applying Wiener Filter Noise Removal. The goal here is to remove noise from the pancreatic CT images; at the same time, to maintain structural detail as well as to preserve important anatomy of the tissues. Following the refinement of images, CLAHE (Contrast-Limited Adaptive Histogram Equalization) is applied to enhance the local contrast of the CT images, which is especially helpful in detecting small structural changes that could be indicative of early pancreatic cancer. Next, TransUNet segmentation is used to segment out the pancreas from the CT images. Combining both CNNs and transformers, TransUNet allows us to correctly identify the location of the pancreas and eliminate all of the unwanted areas. After segmentation, the deep feature extraction has been performed using the NasNet model. Utilizing NasNet's ability to leverage transfer learning, it captures very meaningful and highly discriminating features that illustrate many patterns of different stages of pancreatic cancer. These higher-level features will help to improve the classification results. Finally, after extracting the features, they are fed into a Quasi-Recurrent Neural Network (QRNN) classifier. The QRNN classifier provides a much faster means of modelling sequential dependence and relationships among spatial features. The combination of Convolution Operations and Recurrent Mechanisms provides a significant increase in computational speed as well as better learning of contextual information necessary for accurate staging classification.

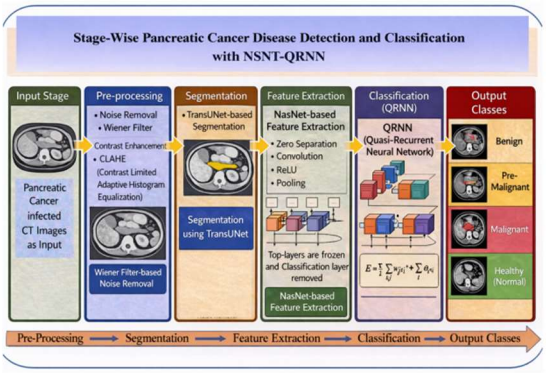

Fig. 1. Overall framework of the Proposed NSNT-QRNN model

3.1 Wiener filter-based noise removal

Computed tomography (CT) scans generate noisy images due to factors associated with image capture, sensor limitations, and transmission. Noise degrades CT scan images. It also obscures small structural changes in pancreatic tissues. A Wiener Filter-based noise reduction process was added at the beginning of the pre-processing, which is an adaptive linear filter that is used to find the minimum Mean Squared Error (MSE) between the original noise-free image and the processed output image. Different from other smoothing-type filters, the Wiener Filter uses the statistics of the image to determine how much smoothing will occur. Therefore, the Wiener Filter smoothes out uniform areas of low variance but preserves high variance areas containing significant detailed borders. The Wiener Filter calculates the local mean and

variance for pixels surrounding a defined neighborhood area for each individual pixel [15]. With this information about the local area, the filter calculates what level of smoothing should be applied to each pixel. Pixels located near highly varied structures (such as anatomical boundaries or pathological regions) have their high variance preserved, whereas pixels found in lower variance locations are smoothed to a greater extent, as depicted in Fig. 2. Due to this adaptive nature, the Wiener Filter is well-suited for medical imaging applications where maintaining structural integrity is extremely important.

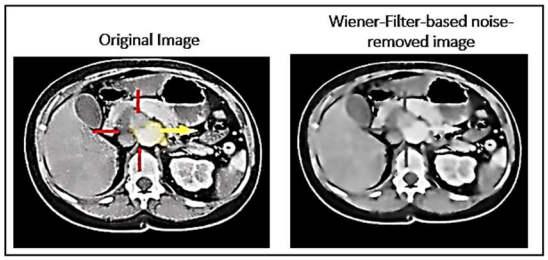

Fig. 2. Wiener-filter-based noise-removed image

The mathematical formulation of the Wiener filter used for image restoration in the spatial domain is given in Eq. (1), where $\hat{f}(x,y)$ represents the restored pixel value, $g(x,y)$ denotes the observed noisy image, μ is the local mean, σ^2 is the local variance, and v^2 is the noise variance:

$$\hat{f}(x,y) = \mu + \frac{\sigma^2 - v^2}{\sigma^2}[g(x,y) - \mu] \quad (1)$$

In addition to the spatial-domain formulation, the Wiener filter can also be expressed in the frequency domain, which provides a more generalized representation of the restoration process. The frequency-domain Wiener filtering is defined in Eq. (2), where $\hat{F}(u,v)$ and $G(u,v)$ represent the restored and degraded images in the frequency domain, respectively, $H(u,v)$ is the degradation function, $H^*(u,v)$ denotes its complex conjugate, and $S_n(u,v)$ and $S_f(u,v)$ correspond to the power spectral densities of the noise and the original image. This formulation enhances restoration performance by incorporating both degradation characteristics and noise statistics in the frequency spectrum.

3.2 CLAHE -based contrast enhancement

Contrast improvement is the subsequent crucial stage after noise removal with the Wiener filter for pre-processing in the suggested NSNT-QRNN framework. The importance of detail enhancement of fine abnormalities or tumour areas in pancreatic CT images lies in the fact that many times, minute intensity differentials are representative of significant pathological changes. Low-contrast and non-uniformly illuminated conditions can limit the ability to see such fine details. To make the details of abnormal tissues more easily visible, it is necessary to enhance the contrast. CLAHE is an enhanced form of contrast enhancement (over histogram-equalized) where, instead of enhancing the whole image (Fig. 3), it enhances each "tile" separately [16]. Histogram equalization (and also CLAHE) have the potential to amplify both high-frequency content and noise in regions of the image where there is little variation. Because CLAHE has a user-defined maximum amount of contrast-stretching before limiting further stretching via clipping the histogram, it has less risk of amplifying noise while still improving local contrast.

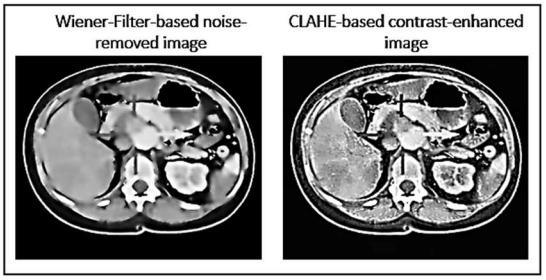

Fig. 3. CLAHE-based contrast-enhanced image

Let $I(x,y)$ denotes the input grayscale image. The image is divided into non-overlapping tiles. T_i , and for each tile, the histogram $H_i(k)$ is computed as shown in Eq. (2), where k represents the intensity level and $\delta(\cdot)$ is the Kronecker delta function.

$$H_i(k) = \sum_{(x,y)\in Ti} \delta(I(x,y) - k) \quad (2)$$

To avoid over-amplification, the histogram is clipped using a clip limit. β as shown in Eq. (3). The excess pixels after clipping are redistributed uniformly across all intensity levels, as shown in Eq. (4), where L is the number of grey levels.

$$H_i^c(k) = \min(H_i(k), \beta) \quad (3)$$

$$H_i^T(k) = H_i^c(k) + \frac{\Sigma_k\left(H_i(k) - H_i^c(k)\right)}{L} \quad (4)$$

$$C_i(k) = \sum_{j=0}^{k} H_i^T(j) \quad (5)$$

$$I'(x,y) = \frac{C_i\big(I(x,y)\big) - C_{i,}min}{(M \times N) - C_{i,}min} \times (L-1) \quad (6)$$

Next, the Cumulative Distribution Function (CDF) for each tile is computed as shown in Eq. (5). The enhanced pixel intensity $I'(x,y)$ is obtained by mapping the original intensity using the normalised CDF as shown in Eq. (6), where $M \times N$ denotes the number of pixels in the tile T_i, and $C_{i,min}$ is the minimum non-zero CDF value.

3.3 TransUNet-based Segmentation

Accurate segmentation of the pancreas using CT scans is an important prerequisite for automating the detection of pancreatic cancer, since this segmentation process isolates the area of interest and removes all extraneous background data. A segmented pancreas with a variable or irregularly shaped geometry and possibly a small size will always be difficult to segment due to its weak contrast. This TransUNet segmentation model employs both Convolutional Neural Network (CNN) and Transformer architectures. While the CNN encoder captures local detail and spatial information, the Transformer component captures long-range dependencies and contextual relationships in the entire image [17], as shown in Fig. 5. The segmentation output is generated as a binary or multiclass mask representing the pancreatic region within the CT image, as depicted in Fig. 4.

Let the input CT image be represented as:

$$X \in \mathbb{R}^{H \times W \times C}$$

The architecture begins with a CNN-based encoder that extracts hierarchical feature representations from the input image, as shown below, where $F_c \in \mathbb{R}^{h \times w \times d}$ denotes the encoded feature map.

$$F_c = \phi_{cnn}(x)$$

These features are then reshaped into a sequence of tokens and embedded with positional information as:

$$Z_0 = \text{Flatten}(F_c) + E_{pos}$$

The Transformer module encodes global contextual relationships using multi-head self-attention as shown in Eq. (7), where $Q = Z_0 W_{Q,} K = Z_0 W_K, and\ V = Z_0 W_V$.

$$Attention(Q,K,V) = Softmax\left(\frac{Qk^T}{\sqrt{d_k}}\right)V \quad (7)$$

The refined feature representation after L Transformer layers are:

$$F_t = Z_L$$

Finally, a decoder reconstructs the segmentation map by combining Transformer features with encoder features through skip connections:

$$F_d = \phi_{\text{lim}}(F_t, F_c)$$

The final segmentation output is obtained by Eq. (8):

$$S(x,y) = Softmax(W_s * F_d + b_s) \quad (8)$$

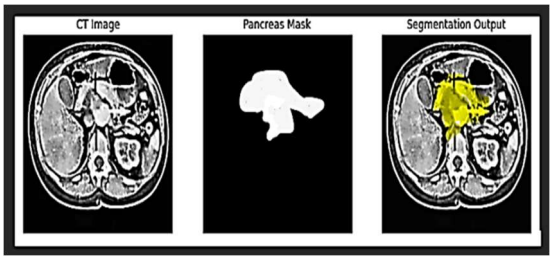

Fig. 4. TransUNet-based segmented CT image along with the Pancreas Mask

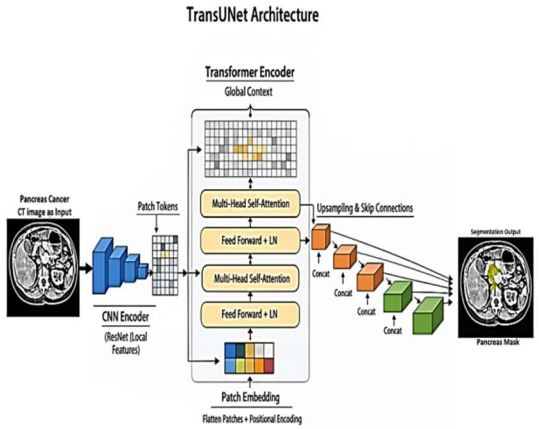

Fig. 5. Architecture of TransUNet-based Segmentation

TransUNet's use of both local feature extraction and global contextual modelling allows it to address variability in the shape, size and intensity of the pancreas. The resulting segmentations

provide an accurate representation of the area of interest (the pancreas) as well as suppression of non-relevant background features. These high-quality segments improve the quality of feature extraction, which in turn improves the overall accuracy of the NSNT-QRNN-based classifier.

3.4 NasNet-based Feature Extraction

After segmentation, Deep Feature Extraction is carried out in order to obtain meaningful and discriminant representations of Pancreatic Tissues. In the proposed NSNT-QRNN framework, the NasNet Model has been used solely as a feature extractor. NasNet (Neural Architecture Search Network) is a state-of-the-art deep learning architecture developed using an automated neural architecture search methodology. This allows for the identification of the most effective convolutional cell structure that will lead to better results than other architectures.

As illustrated in Fig. 6, the segmented pancreatic CT image $X_{seg} \in \mathbb{R}^{224\times224\times3}$ is first passed through a stem convolution block, which consists of a 7×7 convolution with a stride of 2, followed by batch normalization, ReLU activation, and a 3×3 max-pooling operation. This stage performs initial feature extraction and reduces the spatial resolution while increasing the channel operation [18]. This stage performs initial feature extraction and reduces the spatial resolution while increasing channel depth, producing feature maps of sizes $56 \times 56 \times 64$. Subsequently, the feature maps are processed through a sequence of NasNet-A cell blocks, which form the core of the architecture. These blocks are composed of two types of cells, called normal cells and reduction cells. The network follows a repeated pattern of normal cells and reduction cells for the hierarchical arrangement progressively transforms the feature maps from low-level spatial features to high-level semantic representations, with intermediate feature sizes such as $28 \times 28 \times 528$ and $14 \times 14 \times 1056$.

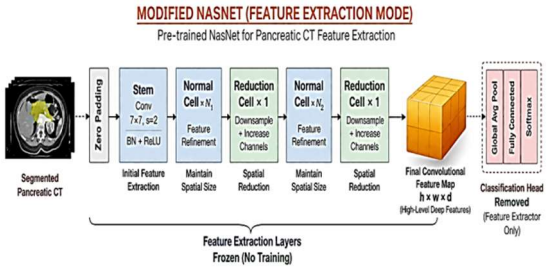

Fig. 6. Architecture of NasNet used for feature extraction

This work utilises a pre-training NasNet Model where all classification head layers (Fully Connected Layers & Softmax) have been removed and replaced with a new feature extraction layer. The new feature extraction layer consists of a single 1x1 Convolutional Layer with 4032 filters, followed by ReLU Activation and Global Average Pooling (GAP). GAP takes spatial feature maps and creates a compact representation of the feature maps by taking the average of each channel in the feature map.

Mathematically, the deep feature extraction process can be expressed as shown in Eq. (9), where $\phi_{nas}(\cdot)$ denotes the feature transformation performed by the modified NasNet, $F_{nas} \in \mathbb{R}^{h\times w\times d}$ is the high-level feature map, and $F_{gap} \in \mathbb{R}^{d}$ is the resulting feature vector after global average pooling as shown in Eq. (10).

$$F_{nas} = \phi_{nas}(X_{seg}) \quad (9)$$

$$F_{gap}(k) = \frac{1}{h\times w}\sum_{i=1}^{h}\sum_{j=1}^{w} F_{\text{nas}}(i,j,k) \quad (10)$$

Finally, the pooled features are then flattened into a single-dimensional vector (4032-Dimensional) and are fed into the QRNN classifier. The top layers of the NasNet model were frozen so that the learned generic features from large-scale datasets can be retained and generalised, and also prevent overfitting to the medical dataset. The deep features that were extracted during this process represent complex characteristics such as texture patterns, structural irregularities, and intensity variability associated with different stages of pancreatic cancer. The representations obtained via deep learning are much more robust, scalable, and discriminant than traditional hand-crafted features, greatly enhancing performance at the next stage, i.e., QRNN-based classification.

3.5 Classification using QRNN

The final stage of the proposed NSNT-QRNN framework is used to classify pancreatic CT images into different stages of cancer severity using a Quasi-RNN as the classifier. This model is a hybrid deep learning approach that combines the advantages of both Convolutional Neural Networks and Recurrent Neural Networks in order to effectively model spatial and temporal relationships within the imaging data [19]. Rather than using

traditional recurrent computations such as those found in traditional RNNs, QRNN uses convolutional operations to capture these relationships. Because convolutional operations allow for parallel processing, they enhance the speed at which QRNN processes high-dimensional deep features extracted from medical imaging data.

Let the deep features extracted from the NasNet model be represented as:

$$X = [x_1, x_2, \dots x_T], \; x_t \epsilon \mathbb{R}^d$$

In this framework, the deep features obtained from the NasNet model are fed into the QRNN classifier. The convolutional layers capture three parallel sequences (Fig. 7), as shown below, where Z_t is the candidate activation, F_t is the forget gate, and O_t is the output gate.

$$Z_t = tanh(W_Z * x_t + b_Z)$$

$$F_t = \sigma(W_f * x_t + b_f)$$

$$O_t = \sigma(W_o * x_t + b_o)$$

The recurrent pooling mechanism models long-range dependencies as:

$$h_t = F_t \odot h_{t-1} + (1\text{-}F_t) \odot Z_t$$

The output at each time is computed as:

$$y_t = O_t \odot h_t$$

The final feature representation is passed to the classification layer as:

$$\hat{y} = Softmax(W_c y_T + b_c)$$

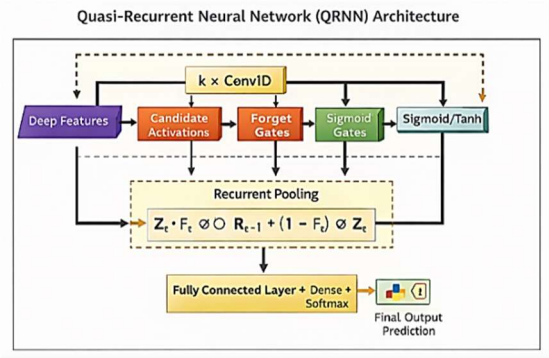

Fig. 7. Architecture of QRNN

This allows the model to successfully classify each stage of pancreatic cancer by identifying small differences in the features for that stage. The QRNN classifier provides a final output for one of the four possible classifications, which are classified as either Healthy (Normal), Benign, Pre-Malignant or Malignant. By utilizing both spatial and context-based information, the QRNN improves the overall accuracy of classification. In general, the QRNN integrated with the NSNT-QRNN framework represents an effective approach for multi-stage diagnosis of pancreatic cancer.

4. EXPERIMENTAL RESULTS

4.1 Implementation Setup

Validation through experimentation was undertaken to assess the efficiency of the proposed NSNT-QRNN-based classification model for detecting stage-wise pancreatic cancer using CT images. Experiments were conducted using a pancreatic CT image dataset that was downloaded from the Kaggle repository [20]. The original dataset consists of 26,400 images categorised into five types: Cancer Stage I, Cancer Stage II, Cancer Stage III, Cancer Stage IV, and Non-Cancer. For this study, four categories of interest were identified: Cancer Stage I, Cancer Stage II, Cancer Stage III, and Non-Cancer. These categories were labelled as follows: Benign, Pre-Malignant, Malignant, and Normal, respectively.

As is evident in Table 1, the original dataset contained an unbalanced number of images across all five classes. Specifically, there were significantly more images available for training and testing in the three classes of interest (Benign, Pre-Malignant, and Malignant) than for the normal class. A total of 2334 images were available for training and testing in the normal class. As a result of the unbalanced nature of the original dataset, a data balancing strategy was employed. An equal number of images were randomly selected from each of the four classes of interest. Specifically, 2330 images were randomly sampled from the Benign, Pre-Malignant, and Malignant classes, and 2330 images were randomly sampled from the normal class. This resulted in a balanced dataset of 9,320 CT images, as is presented in Table 2. Fig. 8 provides a visual representation of the sample images used during the experimentation process.

Table 1. Actual Dataset Details

Class	Number of Samples
Benign	5881
Pre-Malignant	5807
Malignant	5622
Healthy	2334
Total	19,644

Journal of Theoretical and Applied Information Technology
15st July 2026. Vol.104. No.13

ISSN: 1992-8645 www.jatit.org E-ISSN: 1817-3195

Table 2. Balanced Dataset Description

Class	No. of. Samples
Benign	2330
Pre-Malignant	2330
Malignant	2330
Healthy	2330
Total	9320

All experiments were implemented using Python 3.6.5 on a system containing an Intel i5-8600K processor, 16 GB RAM, 250 GB SSD, 1TB HDD, and NVIDIA GeForce GTX 1050 Ti GPU (4 GB). The performance of the proposed model was assessed using traditional measures of classification performance. Such measures include accuracy, sensitivity, specificity, precision, and F-Score.

Table 3. Training Configuration of the Proposed NSNT-QRNN Model

Parameter	Value
Training–Testing Split	70% : 30%
Input Image Size	224 × 224
Optimizer	Adam
Learning Rate	0.001
Batch Size	32
Number of Epochs	50
Loss Function	Categorical Cross-Entropy

Table 3 summarizes the training configuration adopted for the proposed NSNT-QRNN framework. The CT images were resized to 224×224 pixels and divided into training and testing sets using a 70:30 ratio. The model was trained using the Adam optimizer with a learning rate of 0.0001 and a batch size of 32 for 50 epochs. Categorical cross-entropy was employed as the loss function to optimize the multi-class classification process. These settings ensured stable convergence and effective learning of discriminative features for stage-wise pancreatic cancer diagnosis.

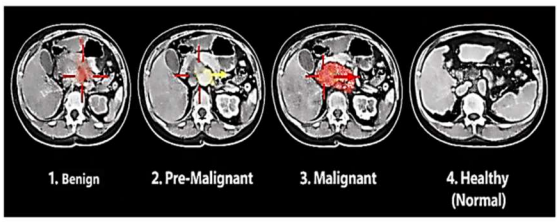

Fig. 8. Sample Dataset Images

4.2 Discussions and Observations

The confusion matrices based on the training (TR) set and testing (TS) set, illustrated in Fig. 9, show that the NSNT-QRNN model performed an effective classification of the four categories (Healthy, Pre-Malignant, Benign, and Malignant) and had a low rate of misclassification. A test set independent from the training set was developed by splitting the data set into 70% for training and 30% for testing. Quantitative results are provided in Table 4, showing that the model can effectively perform stage-wise detection and classification of pancreatic cancer.

The results of the testing phase provided an overall accuracy of 98.90%, an average for precision of 98.60%, an average sensitivity of 98.50%, an average for F-Score of 98.55% and an average for specificity of 99.05%. The above-mentioned metrics further emphasised that the NSNT-QRNN model is highly effective in terms of discrimination. The confusion matrix for testing and training was almost identical to one another, with both indicating a very high amount of correctly classified items. The low amount of incorrectly classified items demonstrated that the NSNT-QRNN model had successfully generalised knowledge from the training dataset. Finally, the Precision-Recall Curve and the ROC Curve also indicated the performance of the NSNT-QRNN model, as it depicted that the model achieved a very high level of precision and recall and that AUC was near to 1.

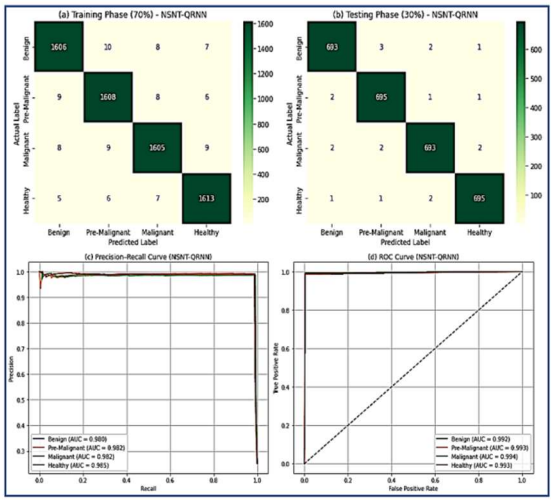

Fig. 9. (a & b) Confusion matrices based on the TR and TS set, (c & d) Precision-Recall and ROC Curves

The NSNT-QRNN model's results are shown in Fig. 10. The model was evaluated on several

parameters, including accuracy, precision, sensitivity, specificity, and F-score for each of the four classes (Benign, pre-malignant, malignant, healthy) used during training (70%). Each class obtained similar results. The results for the benign class obtained an accuracy of 98.70%, a precision of 98.40%, a specificity of 98.90%, a sensitivity of 98.30% and an f-score of 98.35%. The pre-malignant class achieved higher scores than the previous class with an accuracy of 98.90%, a precision of 98.60%, a specificity of 99.00%, a sensitivity of 98.50% and an f-score of 98.55%. In addition, the malignant class had strong scores as well, with an accuracy of 98.80%, a precision of 98.50%, a specificity of 98.90%, a sensitivity of 98.40% and an f-score of 98.45%. However, the health class achieved the highest scores of the four classes with an accuracy of 98.90%, a precision of 98.70%, a specificity of 99.10%, a sensitivity of 98.60% and an f-score of 98.65%. These findings demonstrate that the proposed NSNT-QRNN model demonstrates consistency in terms of all evaluation criteria, as well as demonstrating excellent ability to categorise accurately into their respective groups, and demonstrates its reliability and quality during the training process.

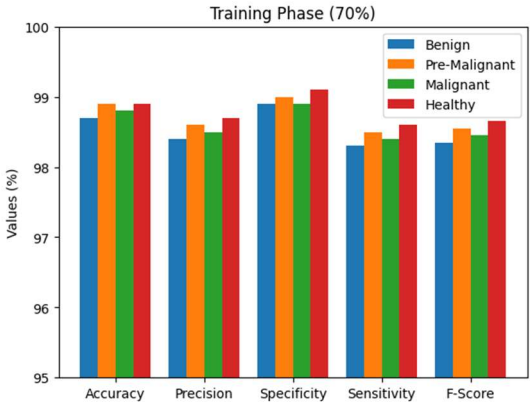

Fig. 10. Graphical representation of the overall outcomes of the NSNT-QRNN model based on the Training phase (70%)

Moreover, the proposed NSNT-QRNN model maintains its good performance during the testing phase (30%), as shown in fig. 11. As seen in fig. 11. During both the training and test phases, the same metrics are applied for evaluating the performance of the model. The Benign Class performed with an accuracy of 98.80%, precision of 98.50%, specificity of 99.0%, sensitivity of 98.40% and f-score of 98.45%. Additionally, the Pre-Malignant Class has better performance than the training phase, with an Accuracy of 99.00%, a Precision of 98.70%, a Specificity of approximately 99.10%, a Sensitivity of 98.40% and an F-Score of 98.45%. While the Malignant Class showed similar performance to the training phase, it had an accuracy of 98.70%, a Precision of 98.40%, a Specificity of 98.90%, a Sensitivity of 98.30% and an F-Score of 98.35%. Once again, the Healthy Class displayed the greatest amount of performance with an accuracy of 99.10%, a precision of 98.80%, a specificity of 99.20%, a sensitivity of 98.70% and an F-Score of 98.75%. Overall, these results demonstrate how reliable and accurate the proposed NSNT-QRNN Model was during the Test Period. Furthermore, the consistently high values for all evaluation metrics also demonstrate how robustly the proposed NSNT-QRNN Model generalized and correctly classified each category.

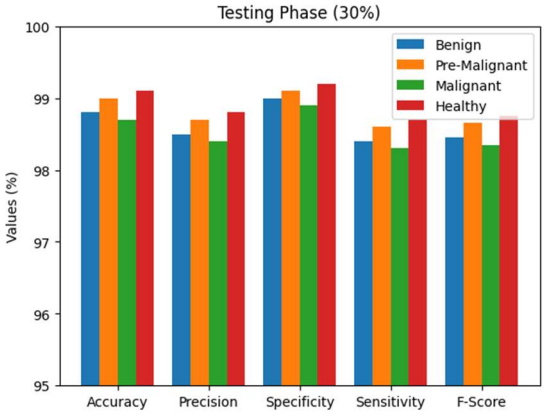

Fig. 11. Graphical representation of the overall outcomes of the NSNT-QRNN model based on the Testing phase (30%)

Table 4. Performance Outcomes of the Proposed NSNT-QRNN Model

Training Phase (70%)					
Class	**Accuracy (%)**	**Precision (%)**	**Specificity (%)**	**Sensitivity (%)**	**F-Score (%)**
Benign	98.70	98.40	98.90	98.30	98.35
Pre-Malignant	98.90	98.60	99.00	98.50	98.55
Malignant	98.80	98.50	98.90	98.40	98.45
Healthy (Normal)	98.90	98.70	99.10	98.60	98.65
Average	98.83	98.55	98.98	98.45	98.50
Testing Phase (30%)					
Class	**Accuracy (%)**	**Precision (%)**	**Specificity (%)**	**Sensitivity (%)**	**F-Score (%)**
Benign	98.80	98.50	99.00	98.40	98.45
Pre-Malignant	99.00	98.70	99.10	98.60	98.65
Malignant	98.70	98.40	98.90	98.30	98.35
Healthy	99.10	98.80	99.20	98.70	98.75

(Normal)					
Average	98.90	98.60	99.05	98.50	98.55

All the current models [21-22] have been less successful than the proposed NSNT-QRNN model, as presented in Table 5. The lowest accuracy rate obtained by the ResNet101 was 83.50%, while the highest one for the ResNeSt was 97.40%. However, the NSNT-QRNN model reached an accuracy of 98.90%, which is clearly the best among those tested. Furthermore, the sensitivity of all the existing models varies from 62.70% up to 91.57%; this is much lower than that of the NSNT-QRNN model with a sensitivity of 97.83%. Therefore, it is evident that the NSNT-QRNN model has a superior capability to identify various states of pancreatic cancer. Additionally, the precision values of all of the above-mentioned models vary from 64.30% up to 94.80%, whereas the precision of the NSNT-QRNN model was 98.60%, indicating that it provides more consistent results. Finally, the F1-scores of all previously reported models range from 63.49% to 92.97%, and the proposed method attained an F1-score of 98.55%, therefore confirming its good balance and high quality in classification performance. It can be easily observed in Fig. 14 how the NSNT-QRNN model outperformed the other methods for each evaluation metric.

Fig. 12 shows that both the Training Accuracy (TACY) and Testing Accuracy (TECY) of the NSNT-QRNN model continuously increase with each additional epoch, indicating that the model continues to identify relevant features in images to detect and distinguish stage-wise pancreatic disease. Although the two curves in Fig. 12 show similar trends of increasing accuracy, most of the time, TECY showed higher values than TACY, thus showing less likelihood of overfitting and high generalization capability. Finally, the model reached its maximum accuracy at the final epoch of training, as evidence that it converged and identified the optimal discriminatory features. Overall, we conclude that NSNT-QRNN demonstrated stable and consistent behaviour during the testing and training processes.

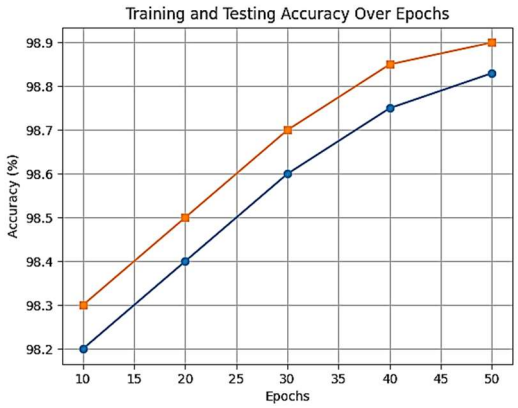

Fig. 12. TACY and TECY of the proposed NSNT-QRNN model

Fig. 13 illustrates the Training Loss (TLOS) and Testing Loss (TELOS) of the NSNT-QRNN model through each epoch. As the number of epochs increases, both TLOS and TELOS decrease steadily, demonstrating the model's ability to learn from data appropriately and achieve convergence. Additionally, TLOS and TELOS are closely aligned, indicating the training stability and no overfitting. Also, the minimum losses occur at the final epoch, demonstrating that the model parameters achieved an optimal configuration. The continued decrease of losses, therefore, demonstrates that NSNT-QRNN is an effective and robust classifier for identifying stage-wise pancreatic cancer diseases.

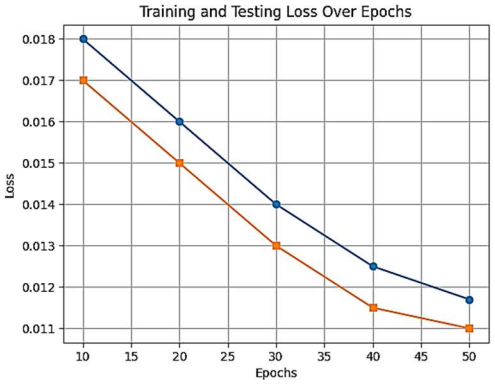

Fig. 13. TLOS and TELOS of the proposed NSNT-QRNN model

Table 5. Comparative Study of the Proposed NSNT-QRNN With Existing Works

Model	Accuracy (%)	Sensitivity (%)	Precision (%)	F-Score (%)
ResNeXt-101	83.50	62.70	64.30	63.49
ResNeSt	84.30	63.20	67.90	65.47

CNN(VGG)	86.70	91.20	88.50	89.83
ResNet 101	90.20	78.60	80.40	79.49
ShuffleNet V2	93.60	90.60	93.90	92.22
CNN	95.47	91.57	93.20	92.38
CNN (DenseNet)	97.40	91.20	94.80	92.97
Proposed NSNT-QRNN	98.90	98.50	98.60	98.55

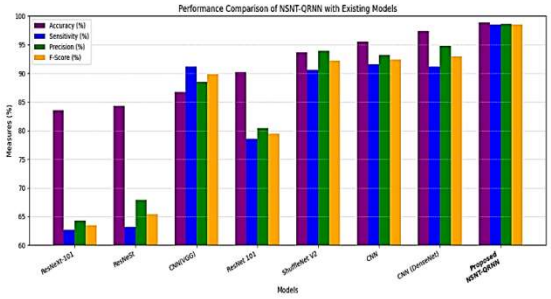

Fig. 14. Graphical representation of Performance comparison of the Proposed NSNT-QRNN with existing works

The ablation study in Table 6 shows how well each component of the NSNT-QRNN model works, since results improve progressively. At first, the baseline QRNN (which has an accuracy of 91.80%), with the addition of a Wiener filter, which will remove noise from images, results in an increase in the accuracy (up to 93.20%). Since removing noise allows us to better see what's going on in an image, this test also confirms how important it is to be able to do so. Then we use CLAHE (Contrast Limited Adaptive Histogram Equalization) to enhance contrasts and emphasise the small details present in the images; CLAHE achieves an accuracy of 94.75%.

Table 6. Ablation Study of the Proposed NSNT-QRNN

Configuration	Wiener Filter	CLAHE	TransUNet Segmentation	NasNet Feature Extraction	Classifier	Accuracy (%)
Baseline (QRNN only)	✗	✗	✗	✗	QRNN	91.80
+ Wiener Filter	✓	✗	✗	✗	QRNN	93.20
+ Wiener + CLAHE	✓	✓	✗	✗	QRNN	94.75
+ Wiener + CLAHE + TransUNet	✓	✓	✓	✗	QRNN	96.30
+ Wiener + CLAHE + TransUNet + NasNet	✓	✓	✓	✓	QRNN	97.80
Proposed NSNT-QRNN (Full Pipeline)	✓	✓	✓	✓	QRNN	98.90

The introduction of TransUNet, which segments the images and eliminates the background, provides the most significant performance boost (to 96.30%) because this process correctly identifies the area of interest. Next, incorporating NasNet-based feature extraction into the model provides another increase in performance (the accuracy reaches 97.80%) as these models can extract very complex and discriminant characteristics from images. Finally, when all components are used together in the complete NSNT-QRNN model, it produces the best results (accuracy=98.90%), and thus validates the efficiency of the proposed methodology as well as its robustness.

4.3. Difference from Prior Research and Research Contributions

Unlike many existing studies that mainly focus on binary pancreatic cancer classification, the proposed NSNT-QRNN framework performs stage-wise classification into Healthy, Benign, Pre-Malignant, and Malignant categories. The framework integrates TransUNet-based segmentation for accurate pancreas localization, NasNet for discriminative feature extraction, and QRNN for efficient classification. Experimental results demonstrate that the proposed model achieves superior performance, attaining 98.90% of accuracy, 98.60% of precision, 98.50% of sensitivity, and 98.55% of F-score compared with recent state-of- the- art approaches. These findings confirm the effectiveness of the proposed framework for automated stage-wise pancreatic cancer diagnosis. However, further validation on longer multi-center datasets is required to enhance generalizability and clinical applicability.

5. CONCLUSION

This study addressed the research problem of developing an automated and accurate framework for stage-wise pancreatic cancer detection using CT images. The proposed NSNT-QRNN framework integrates advanced image enhancement, pancreas segmentation, deep feature exraction, and classification techniques within a unified architecture. The experimental findings confirm

that the proposed NSNT-QRNN approach, achiving an accuracyof 98.90%, precision of 98.60%, sensitivity of 98.50%, specificity of 99.05%, and F-score of 98.55%, thereby outperforming several existing methods. Furthermore, the ablation study confirmed that each component of the framework contributed positively to the overall classification performance. The study objectives of accurate pancreas localization, discriminative feature learning, and reliable stage-wise pancreatic cancer classification were successfully achieved. These findings highlight the potential of the proposed NSNT_QRNN framework as an effective decision-support tool for pancreatic cancer diagnosis. However, the present study has certain limitations. The proposed framework was evaluated using a single publicly available dataset, which may limit its generalizability to diverse clinical environments. In addition, the computational complexity associated with the integrated TransUNet and NasNet architectures may present challenges for deployment in resource-constrained health-care frameworks.

6. OPEN CHALLENGES AND FUTURE WORKS

Although the proposed NSNT-QRNN framework has shown great potential in detecting and classifying pancreatic cancer, there are still many issues that have yet to be addressed. The first issue relates to how to evaluate the model. The model is evaluated based on a small dataset and therefore needs to test the model's ability to generalize using larger and more varied datasets from multiple clinical facilities. The second issue relates to increased complexity in computation due to the combination of TransUNet-based segmentation and NasNet-based features. This could result in longer times to train the model and require greater resources, possibly preventing the use of this model in real-time clinical settings. A third major issue exists related to the variation in image quality and variability in CT images, specifically the level of noise, resolution difference, and variation in imaging protocols used at different scanner locations. Finally, an additional significant challenge exists related to the interpretability of deep learning models. As mentioned previously, since the NSNT-QRNN framework includes multiple layers of deep architecture, it acts as a "black box", and as a result, it is difficult for medical professionals to completely trust and understand the decisions made by the model. Future research will focus on optimizing the NSNT-QRNN framework for real-time clinical use by decreasing the computational complexity and developing lighter-weight architectures. In addition, XAI techniques will be integrated into the framework to increase model transparency and trustworthiness. The NSNT-QRNN framework can also be expanded upon to include multi-modality medical imaging data, i.e., integrating CT with MRI scans, etc., in order to increase the diagnostic accuracy of the model. Future studies will also focus on developing models capable of identifying and distinguishing between various stages of pancreatic cancer, and validating these models in actual clinical settings to assess their robustness and utility.

REFERENCES

[1] M. Costache, C. A. Costache, C. I. Dumitrescu, A. Tica, M. Popescu, E. A. Baluta, A. C. Anghel, A. Saftoiu and D. Dumitrescu, "Which is the Best Imaging Method in Pancreatic Adenocarcinoma Diagnosis and Staging - CT, MRI or EUS?," Current Health Sciences Journal, vol. 43, no. 2, pp. 132-236, 29 June 2017.

[2] P. Rawl, T. Sunkara and V. Gaduputi, "Epidemiology of Pancreatic Cancer: Global Trends, Etiology and Risk Factors," World Journal of Oncology, vol. 10, no. 1, pp. 10-27, 26 February 2019.

[3] A. Jemal, R. Siegel, E. Ward, T. Murray, J. Xu, C. Smigal and M. J. Thun, "Cancer statistics, 2006," A Cancer J Clin, vol. 56, no. 2, pp. 106-30, MarchApril 2006.

[4] R. Siegel, D. Naishadham and A. Jemal, "Cancer statistics, 2012," CA Cancer J Clinic, vol. 62, no. 1, pp. 10-29, January-February 2012.

[5] K.-L. Liu, T. Wu, P.-T. Chen, Y. M. Tsai, H. Roth, M.-S. Wu, W.-C. Liao and W. Wang, "Deep learning to distinguish pancreatic cancer tissue from noncancerous pancreatic tissue: a retrospective study with cross-racial external validation," Lancet Digit Health, vol. 2, no. 6, pp. e303-e313, June 2020.

[6] M. ROBERT FREELOVE and M. C. ANNE D. WALLING, "Pancreatic Cancer: Diagnosis and Management," Am Fam Physician, vol. 73, no. 3, pp. 485-492, 2006.

[7] Ramesh, J. V. N., Abirami, T., Gopalakrishnan, T., Narayanasamy, K., Ishak, M. K., Karim, F. K., Mostafa, S. M., & Allakany, A. (n.d.). Sparrow Search Algorithm With Stacked Deep Learning Based Medical Image Analysis for Pancreatic Cancer

Detection and Classification. *IEEE Access*, *11*, 111927–111935. https://doi.org/10.1109/access.2023.3322376.

[8] Dodda, K., & Muneeswari, G. (2025). Automatic pancreatic cancer segmentation and classification in CT images using an integrated deep-learning approach. *PeerJ*, *11*, e3263. https://doi.org/10.7717/peerj-cs.3263.

[9] Khair, F. B., Saimon, A. S. M., Hossain, S., Manik, M. M. T. G., Ahmed, M. K., Islam, Md. S., & Moniruzzaman, M. (2025). Deep neural network-based imaging system for efficient pancreatic tumor identification. *Intelligent Decision Technologies*. https://doi.org/10.1177/18724981251381581.

[10] Khdhir, R., Belghith, A., & Othmen, S. (2023). Pancreatic Cancer Segmentation and Classification in CT Imaging using Antlion Optimization and Deep Learning Mechanism. *International Journal of Advanced Computer Science and Applications*, *14*(3). https://doi.org/10.14569/ijacsa.2023.0140307.

[11] Gomathi, P. (2025). Pancreatic Cancer Classification Based on Deep Learning. *Journal of Information Systems Engineering and Management*, *10*(3), 780–788. https://doi.org/10.52783/jisem.v10i3.6223.

[12] Mitrea, D., Brehar, R., Itu, R., Nedevschi, S., Socaciu, M., & Badea, R. (2024). *Pancreatic Tumor Recognition from CT Images through Advanced Deep Learning Techniques*. https://doi.org/10.1109/aqtr61889.2024.10554139.

[13] Shnawa, A. H., Mohammed, G., Hadi, M. R., Ibrahim, K., Adnan, M. M., & Hameed, W. (2023). *Optimal Elman Neural Network for Pancreatic Cancer Classification Using Computed Tomography Images*. 689–695. https://doi.org/10.1109/iiceta57613.2023.10351360.

[14] Si, K., Xue, Y., Yu, X., Zhu, X., Li, Q., Gong, W., Liang, T., & Duan, S. (2021). Fully end-to-end deep-learning-based diagnosis of pancreatic tumors. *Theranostics*, *11*(4), 1982–1990. https://doi.org/10.7150/THNO.52508.

[15] Balakrishna, R., & Anandan, R. (2020). Feature Classification and Analysis of Acute and Chronic Pancreatitis Using Supervised Machine Learning Algorithm. In *Intelligent Computing in Engineering: Select Proceedings of RICE 2019* (pp. 241-249). Singapore: Springer Singapore.

[16] Chaithanyadas, K. V., & Gnana King, G. R. (2023). Detection of pancreatic tumor from computer tomography images using 3D convolutional neural network. In *Computational Vision and Bio-Inspired Computing: Proceedings of ICCVBIC 2022* (pp. 289-303). Singapore: Springer Nature Singapore.

[17] de Paiva, F. F., de Carvalho Araújo, A., de Almeida, J. D. S., & de Paiva, A. C. (2025). Pancreatic Mass Segmentation Using TransUNet Network. In *ICEIS (1)* (pp. 512-522).

[18] Chhikara, J., Goel, N., & Rathee, N. (2025). Integrating expert guidance with gradual moment approximation (GMAp)-enhanced transfer learning for improved pancreatic cancer classification. *Neural Computing and Applications*, *37*(3), 1357-1373.

[19] Xuan, W., & You, G. (2020). Detection and diagnosis of pancreatic tumor using deep learning-based hierarchical convolutional neural network on the internet of medical things platform. *Future Generation Computer Systems*, *111*, 132-142.

[20] Pancreatic Dataset: https://www.kaggle.com/datasets/mdismailbhuiyan/pancreatic-cancer-dataset-input

[21] Huy, H. Q., Dat, N. T., Hiep, D. N., Tram, N. N., Vu, T. A., & Huong, P. T. V. (2023). *Pancreatic Cancer Detection Based on CT Images Using Deep Learning* (pp. 66–72). Springer International Publishing. https://doi.org/10.1007/978-981-99-4725-6_10.

[22] Nadeem, A., Ashraf, R., Mahmood, T., & Perveen, S. (2025). Automated CAD system for early detection and classification of pancreatic cancer using deep learning model. *PLOS ONE*, *20*(1), e0307900. https://doi.org/10.1371/journal.pone.0307900